REGULARIZED SHAPE DEFORMATION FOR IMAGE SEGMENTATION

Song Wang and Zhi-Pei Liang

Beckman Institute and ECE Department
University of Illinois at Urbana-Champaign, IL 61801
songwang, z-liang@uiuc.edu

Abstract

This paper presents a new method for image segmentation by deforming the object shape in a template. The deformation process is controlled using a thin-plate spline kernel based regularization method. The proposed method is especially useful for 2D-based segmentation of 3D medical images by treating segmented slices as templates for their neighboring unsegmented slices. We have applied the proposed method to extract the scalp contours in brain cryosection images with very encouraging results.

1. INTRODUCTION

An effective way for image segmentation is to incorporate the known shape information of the desired objects into the segmentation process. Generally, the shape of an object is described by the boundary contour (or several closed contours) of the object, which can be represented by a sequence of sampled landmark points.

A number of shape-based segmentation methods have been proposed. For example, the active contour (or snakes) [1] model constrains the desired shape to be sufficiently continuous, smooth and differentiable during the deformation process. Although the original active contour cannot process multiple contours, the problem can be solved using the recent geodesic contour method [2].

More advanced shape models include the point distribution model (PDM) by Cootes et al.[3], which can learn shape variations from a set of segmented training images, containing a set of landmarks to define the shape. PDM calculates the covariance matrix of these landmarks and then the shape variations are represented along the directions of the most significant eigenvectors of the covariance matrix. However, it is a tedious job to build the training set manually and in some cases it is difficult to identify the corresponding landmark set for all the shapes. Similarly to PDM, Staib et al. [4] decompose the shape into items with different frequencies. Then the shape knowledge is learned through studying the distribution of each Fourier coefficient. The result is used to constrain the shape deformation. Jain [5] also proposed a similar approach which uses a parametric shape model to consider shape deformation.

In this paper, we present a shape deformation method taking advantage of the special characteristics of medical images. Specifically, we treat 3D medical images as a sequence of 2D slices. We first manually segment one or a few slices to construct the initial templates. The object shapes in these templates are then deformed to segment their neighboring slices one at a time until all the slices are successfully segmented. In the process, the template is successively updated before it is used to process the adjacent slice.

The rest of the paper is organized as follows. In section 2, we describe the shape-based deformation method based on the thin-plate regularizations. Section 3 presents some of its applications to medical image segmentation, followed by the conclusion in section 4.

2. THE PROPOSED METHOD

For simplicity, consider the case in which the template image contains only a single closed contour. Extension to multiple contours is straightforward. Here the contour is represented as a series of ordered landmark points $\mathbf{V} = \{\mathbf{v}_1, \mathbf{v}_2, ..., \mathbf{v}_n\}$, where $\mathbf{v}_i = (x_i, y_i)$ are the coordinates of the i-th landmark. The proposed method first identifies a set of corresponding landmark points $\mathbf{V}' = \{\mathbf{v}'_1, \mathbf{v}'_2, ..., \mathbf{v}'_n\}$ where $\mathbf{v}'_i = (x'_i, y'_i)$ are obtained from the target image using conventional edge detection algorithms. With the detected (noised) landmarks $\mathbf{V}'$, the next step is to deform the shape $\mathbf{V}$ to match $\{\mathbf{v}'_1, \mathbf{v}'_2, ..., \mathbf{v}'_n\}$ while also keeping the general shape characteristics of $\mathbf{V}$. This can be described as a regularization problem as finding $\mathbf{T} = (f, g) : \mathbf{R}^2 \rightarrow \mathbf{R}^2$ that minimizes

$$\frac{1}{n}\sum_{i=1}^{n} \|\mathbf{v}'_i - \mathbf{T}(\mathbf{v}_i)\|^2 + \lambda\phi[\mathbf{T}] \qquad (1)$$

where $\lambda \geq 0$ is a regularization factor and $\phi[\mathbf{T}] \geq 0$ is the desired regularization. There are three main steps in our approach: detecting $\mathbf{V}'$, selecting of $\phi[\mathbf{T}]$ and calculating λ, which are discussed below.

2.1. Extraction of $\mathbf{V}'$

With $\mathbf{V}$ as an initial estimate, we assume that $\mathbf{v}_i'$ falls inside a circle $R(\mathbf{v}_i)$ centered at $\mathbf{v}_i$ with radius r_i in the target image. Within $R(\mathbf{v}_i)$, all the candidate "edge" points are identified based on the pixel intensity gradient, and the one with the largest intensity gradient amplitude is chosen as landmark $\mathbf{v}_i'$. Selection of r_i is related to the similarity between the template and the target. For segmenting 3D medical images slice by slice, this is usually determined by the distance between two neighboring slices. The larger the distance, the larger the r_i. In practice, r_i should be adaptively modified based on the number of the candidate edge points in $R(\mathbf{v}_i)$. If there are too many candidate edge points in $R(\mathbf{v}_i)$, then r_i needs to be reduced, and vice versa. In practice, because an overestimated r_i may introduce some edge points from other structures, an upper limit for r_i is often set. Sometimes, for computational efficiency, we only search for the corresponding landmark $\mathbf{v}_i'$ along the normal direction of $\mathbf{v}_i$ instead of from all pixels in $R(\mathbf{v}_i)$ as shown in Fig.1.

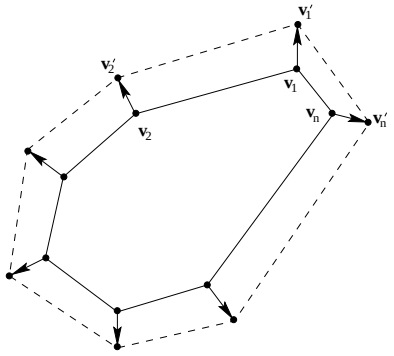

Fig. 1. Search for landmarks along the normal direction of the initial shape.

It is possible that no landmark points are identified in some areas $R(\mathbf{v}_i)$ because of noise or occlusion. However, this is not a problem in the proposed method because with the proposed method discussed in the next section, we can use only the remaining landmarks detected in the target image to determine the shape deformation function. With this function, the undetected landmarks can be calculated directly. This is desirable because we can purposely remove some detected landmarks that are suspected to be incorrect so that the influence of noise and edge detection errors can be kept small.

2.2. Regularization

From the regularization theory, $\phi[\mathbf{T}]$ can be defined as a norm in a reproducing kernel Hilbert space (or subspace) which can be uniquely represented by a positive definite (or conditionally positive definite) kernel function $K(\mathbf{v}, \mathbf{v}')$. For the medical image segmentation, the desired transform T should be a homologous mapping geometrically and well reflect the biologic shape deformation. For our problem, we propose to use the thin-plate kernel $K(\mathbf{v}, \mathbf{v}') = \|\mathbf{v} - \mathbf{v}'\|^2 \log \|\mathbf{v} - \mathbf{v}'\|$ [6], where $\phi[\mathbf{T}]$, also named the *bending energy*, is given by

$$\phi[\mathbf{T}] = \int \int_{-\infty}^{\infty} (L(f) + L(g)) dxdy \tag{2}$$

where $L(\cdot) = (\frac{\partial^2}{\partial x^2})^2 + 2(\frac{\partial^2}{\partial x \partial y})^2 + (\frac{\partial^2}{\partial y^2})^2$.

According to the splines theory [7], the solution of the thin-plate regularization can be acquired by

$$\begin{aligned} f(\mathbf{v}) &= a_1 + a_2 x + a_3 y + \sum_{i=1}^{n} c_i K(\mathbf{v}, \mathbf{v}_i) \\ g(\mathbf{v}) &= b_1 + b_2 x + b_3 y + \sum_{i=1}^{n} d_i K(\mathbf{v}, \mathbf{v}_i). \end{aligned} \tag{3}$$

Here $\mathbf{v} = (x, y)$ and $K(\cdot, \cdot)$ is the thin-plate kernel and the parameters $\mathbf{a} = (a_1, a_2, a_3)^T$, $\mathbf{b} = (b_1, b_2, b_3)^T$, $\mathbf{c} = (c_1, c_2, ..., c_n)^T$ and $\mathbf{d} = (d_1, d_2, ..., d_n)^T$ are calculated by

$$\begin{pmatrix} \mathbf{K} + n\lambda\mathbf{I} & \mathbf{P} \\ \mathbf{P}^T & \mathbf{0} \end{pmatrix} \begin{pmatrix} \mathbf{c} & \mathbf{d} \\ \mathbf{a} & \mathbf{b} \end{pmatrix} = \begin{pmatrix} \mathbf{x}' & \mathbf{y}' \\ \mathbf{0} & \mathbf{0} \end{pmatrix} \tag{4}$$

where $k_{ij} = K(\mathbf{v}_i, \mathbf{v}_j); i, j = 1, 2, ..., n$ are the elements of matrix $\mathbf{K}$ and $\mathbf{P} = (\mathbf{1}, \mathbf{x}, \mathbf{y})$. Here $\mathbf{x} = (x_1, x_2, ..., x_n)^T$, $\mathbf{y} = (y_1, y_2, ..., y_n)^T$, $\mathbf{x}' = (x_1', x_2', ..., x_n')^T$ and $\mathbf{y}' = (y_1', y_2', ..., y_n')^T$.

With the thin-plate regularization method, we get a new regularized shape $\mathbf{T}(\mathbf{V})$. It is obvious that when $\lambda = 0$, it degenerates to the popular thin-plate interpolation method [6], in which the deformed shape is the same as the detected $\mathbf{V}'$. In the other extreme, if $\lambda = \infty$, the thin-plate regularization attempts to find the best affine transform on $\mathbf{V}$ which has least square error with $\mathbf{V}'$ since now the solution must be in the space $\{f | L(f) = 0\}$. That means that, with the thin-plate regularization, the shape is considered to be invariant under the affine transform.

2.3. Selection of λ

The regularization parameter λ plays an important role in the thin-plate deformation. The optimal λ is chosen for our problem by minimizing the ordinary cross-validation (OCV) function

$$V_0(\lambda) = \frac{1}{n} \sum_{i=1}^{n} [(x_i' - f^{[k]}(\mathbf{v}_i))^2 + (y_i' - g^{[k]}(\mathbf{v}_i))^2]$$

where $f^{[k]}$ and $g^{[k]}$ are the minimizers of the following two functions, respectively,

$$\frac{1}{n}\sum_{i=1,i\neq k}^{n}(x_i' - f(\mathbf{v}_i))^2 + \lambda\int\int_{-\infty}^{\infty} L(f)dxdy$$
$$\frac{1}{n}\sum_{i=1,i\neq k}^{n}(y_i' - g(\mathbf{v}_i))^2 + \lambda\int\int_{-\infty}^{\infty} L(g)dxdy.$$

They are solved from (4) for a set of λ. In fact, this is acquired using the principle of "leaving-out-one" cross-values for cross validation.

Wahba [7] have conducted a thorough study on how to estimate λ for the scalar function approximation splines and also generate the OCV to generalized cross validation (GCV). The main principle can also be adapted to select optimal λ for our 2D shape deformation problem here.

3. EXPERIMENTS

The proposed regularization method has been used to extract the scalp contour from a series of brain cryosection images from the Visual Human Project. Fig.2 shows the initial template slice with manual extracted scalp contour consisting of 100 landmark points distributed uniformly.

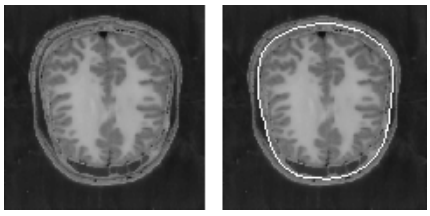

Fig. 2. Left: initial template image; Right: the manually extracted scalp contour.

According to section 2.1, we extract $\mathbf{V}'$ along the normal direction of the template shape. For scalp contours in cryosection image, it is easy to see that the intensity of pixels just outside the scalp contour is smaller than of those just inside the contour. So the extraction of the landmarks $\mathbf{v}_i'$ is done by searching the a rising-edge (from outside to inside) near $\mathbf{v}_i$ and along the normal direction centered at $\mathbf{v}_i$.

To demonstrate the performance of the proposed shape deformation method, a set of result is shown in Fig.3, where the template and target images are separated by five or ten slices. As can be seen, the proposed shape deformation method can get the scalp contour quite accurately even with inaccurate edge points detected from the target image. For practical applications, where a target is the neighbor of the template, the geometric difference between the template and the target images is much smaller, and we can expect much better result.

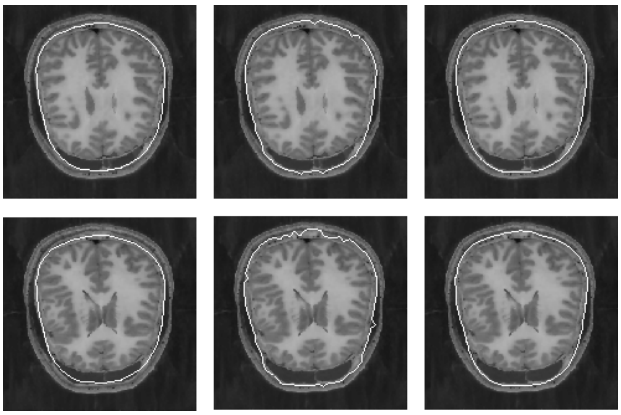

Fig. 3. The result of the shape deformation. The target image in the top row is 5 slices away from the template; the image in the bottom row is 10 slices away from the template. The left column is the initial template shape superimposed in the target image; the middle column is the detection of the landmarks; the right column is the deformed shape.

Finally, we use the proposed deformation method to segment the scalp contour from a 3D cryosection brain image. Fig.4 is the segmentation of the slices above the template slice while Fig.5 is the results for slices below the template in the 3D brain cryosection image. Both the first image in Fig.4 and last image in Fig.5 are 31 slices away from the initial template image. The result is considered very good given the difficulty in extracting the scalp contour.

Another desirable property of the proposed method is its flexibility in selecting the landmarks. In the PDM model, all the shapes should have the same number of landmarks and there exists an one-to-one landmark correspondence between every two shapes. In the proposed method, this is required only between the neighbors (the template and the target images). After the shape deformation, we can re-sample the shape contour in a slice before it is used as the template to segment its neighbors. This is very useful in practical application since after the shape deformation, the landmarks may be overly redundant in some segments and too sparse in other segments along the contour.

4. CONCLUSION

This paper presents an image segmentation method using shape regularization. This method is especially suitable for segmenting 3D medical images slice by slice, where there are only small shape variation across the neighboring slices. The segmented shape in one slice can be used as a template for its unsegmented neighbors.

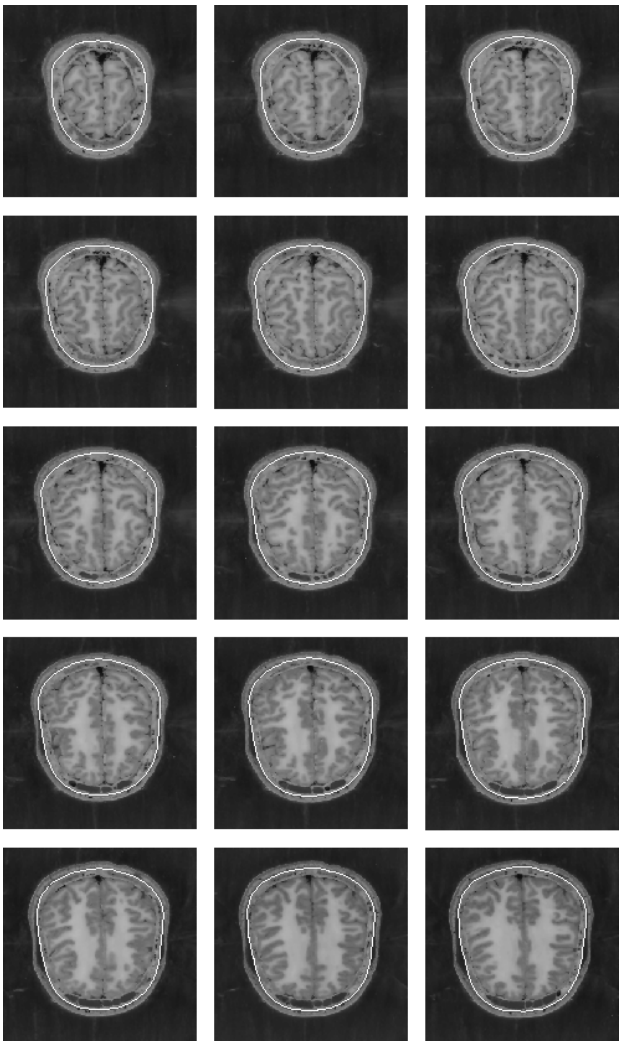

Fig. 4. Segmentation of the slices above the template. The top-left one is 31 slices away from the template; The bottom-right one is 1 slice away from the template.

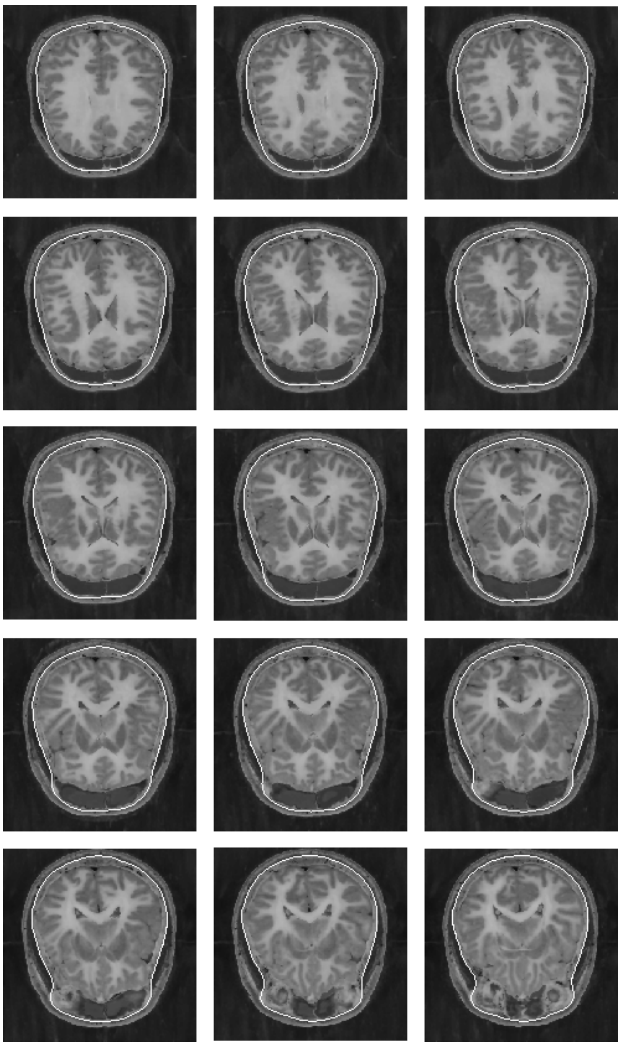

Fig. 5. Segmentation of the slices below the template.The top-left one is 1 slice away from the template; The bottom-right one is 31 slices away from the template.

5. REFERENCES

[1] M. Kass, A. Witkin, and D. Terzopoulos, "Snakes: Active contour models," in *Int. Journal of Computer Vision*, vol. 1(4), pp. 321–331, 1987.

[2] V. Casselles, F. Catte, T. Coll, and F. Dibos, "A geometric model for active contours," *Numerische Mathematik*, vol. 66, pp. 1–31, Jan. 1993.

[3] T. F. Cootes, C. J. Taylor, D. H. Cooper, and J. Graham, "Active shape models - their training and application," *Computer Vision and Image Understanding*, vol. 61, pp. 38–59, Jan. 1995.

[4] L. H. Staib and J. S. Ducan, "Boundary finding with parametrically deformable models," *IEEE Trans. PAMI*, vol. 17, pp. 1061–1075, Nov. 1992.

[5] A. K. Jain, Y. Zhong, and S. Lakshmanan, "Object matching using deformable templates," *IEEE Trans. PAMI*, vol. 18, pp. 267–278, March 1996.

[6] F. L. Bookstein, "Principal warps: Thin-plate splines and the decomposition of deformations," *IEEE Trans. PAMI*, vol. 11, pp. 567–585, June 1989.

[7] G. Wahba, *Spline Models for Observational Data*. Society Industrial and Applied Mathematics, 1990.